European Journal of Neuroscience, Vol. 11, pp. 3499–3511, 1999

Differential regulation of tyrosine hydroxylase in the basal ganglia of mice lacking the dopamine transporter

Mohamed Jaber, Brigitte Dumartin, Corinne Sagné,[1] John W Haycock,[2] Christine Roubert,[1] Bruno Giros,[1] Bertrand Bloch and Marc G. Caron[3]

CNRS UMR 5541, Université Bordeaux II Victor Segalen, 146 rue Léo Saignat, 33076 Bordeaux Cedex, France
[1]INSERM U-288, 91 Boulevard de l'Hôpital, 75013 Paris, France
[2]Louisiana State University, Dept. of Biochemistry and Molecular Biology, New Orleans, LA 70119, USA
[3]Howard Hughes Medical Institute Laboratories, Departments of Cell Biology and Medicine, Duke University Medical Center, Durham, NC 27710 USA

Keywords: DOPA decarboxylase, immunohistochemistry, knock-out, vesicular monoamines transporter

Abstract

Mice lacking the dopamine transporter (DAT) display biochemical and behavioural dopaminergic hyperactivity despite dramatic alteration in dopamine homeostasis. In order to determine the anatomical and functional integrity of the dopaminergic system, we examined the expression of tyrosine hydroxylase (TH), the rate-limiting enzyme of dopamine synthesis as well as DOPA decarboxylase and vesicular monoamine transporter. TH-positive neurons in the substantia nigra were only slightly decreased (–27.6 ± 4.5%), which can not account for the dramatic decreases in the levels of TH and dopamine that we previously observed in the striatum. TH mRNA levels were decreased by 25% in the ventral midbrain with no modification in the ratio of TH mRNA levels per cell. However, TH protein levels were decreased by 90% in the striatum and 35% in the ventral midbrain. In the striatum, many dopaminergic projections had no detectable TH, while few projections maintained regular labelling as demonstrated using electron microscopy. DOPA decarboxylase levels were not modified and vesicular transporter levels were decreased by only 28.7% which suggests that the loss of TH labelling in the striatum is not due to loss of TH projections. Interestingly, we also observed sporadic TH-positive cell bodies using immunohistochemistry and *in situ* hybridization in the striatum of homozygote mice, and to some extent that of wild-type animals, which raises interesting possibilities as to their potential contribution to the dopamine hyperactivity and volume transmission previously reported in these animals. In conjunction with our previous findings, these results highlight the complex regulatory mechanisms controlling TH expression at the level of mRNA, protein, activity and distribution. The paradoxical hyperdopaminergia in the DAT KO mice despite a marked decrease in TH and dopamine levels suggests a parallel to Parkinson's disease implying that blockade of DAT may be beneficial in this condition.

Introduction

The dopamine transporter (DAT) is a plasma membrane protein that is responsible for terminating neurotransmission by rapid re-uptake of dopamine (Giros *et al*., 1991; Giros & Caron, 1993). We have developed a strain of mice lacking the DAT ($DAT^{-/-}$) by homologous recombination (Giros *et al*., 1996). $DAT^{-/-}$ mice present a hyperactive dopamine phenotype that is reflected behaviourally by the increase in the spontaneous locomotor activity. Extracellular dopamine levels were found to be five times that of control, and dopamine clearance is prolonged at least 300 times. The excess dopamine activity caused by the transporter inactivation is partially offset by a substantial decrease in the amount of dopamine available for release (Jones *et al*., 1998). Furthermore, these animals show a 50% downregulation of both D1 and D2 receptors, the main dopaminergic receptors in dopaminoceptive neurons of the basal ganglia. Additionally, presynaptic D2 receptors are downregulated and autoreceptor control of dopamine release is severely impaired in these animals (Jones *et al*., 1999). However, all these adaptive responses do not restore the striatum to normal functioning and fail to compensate for the inactivation of the DAT. The huge decrease in striatal intracellular dopamine (95%) was found to be associated with a decrease in tyrosine hydroxylase (TH) [L-tyrosine, tetrahydropteridine:oxygen oxidoreductase (3-hydroxylating), EC 1.14.16.2], which is the rate-limiting enzyme of dopamine biosynthesis (Nagatsu *et al*., 1964; Levitt *et al*., 1965). These results were obtained from striatal extracts using Western blot. Surprisingly, striatal dopamine synthesis rates were doubled suggesting that TH activity was significantly and dramatically increased (Jones *et al*., 1998). Indeed, the reduced number of TH molecules present in $DAT^{-/-}$ mice seem to function at a much higher rate than those present in normal animals.

The above alterations in dopamine homeostasis call into question the integrity and the neuroanatomy of the dopamine system in the basal ganglia of $DAT^{-/-}$ mice. In addition, a detailed characterization of the dopamine system in these animals is crucial to better understand the implication of the DAT in drug addiction (Beatriz *et al*., 1998), attention deficit disorder (Gainetdinov *et al*., 1999), MPTP neurotoxicity and Parkinson's disease (Gainetdinov *et al*., 1997; Jaber *et al*., 1997; Bezard *et al*.,

Correspondence: Dr M. Jaber, as above.
E-mail: mjaber@hippocrate.u-bordeaux2.fr

Received 8 March 1999, revised 17 May 1999, accepted 24 May 1999

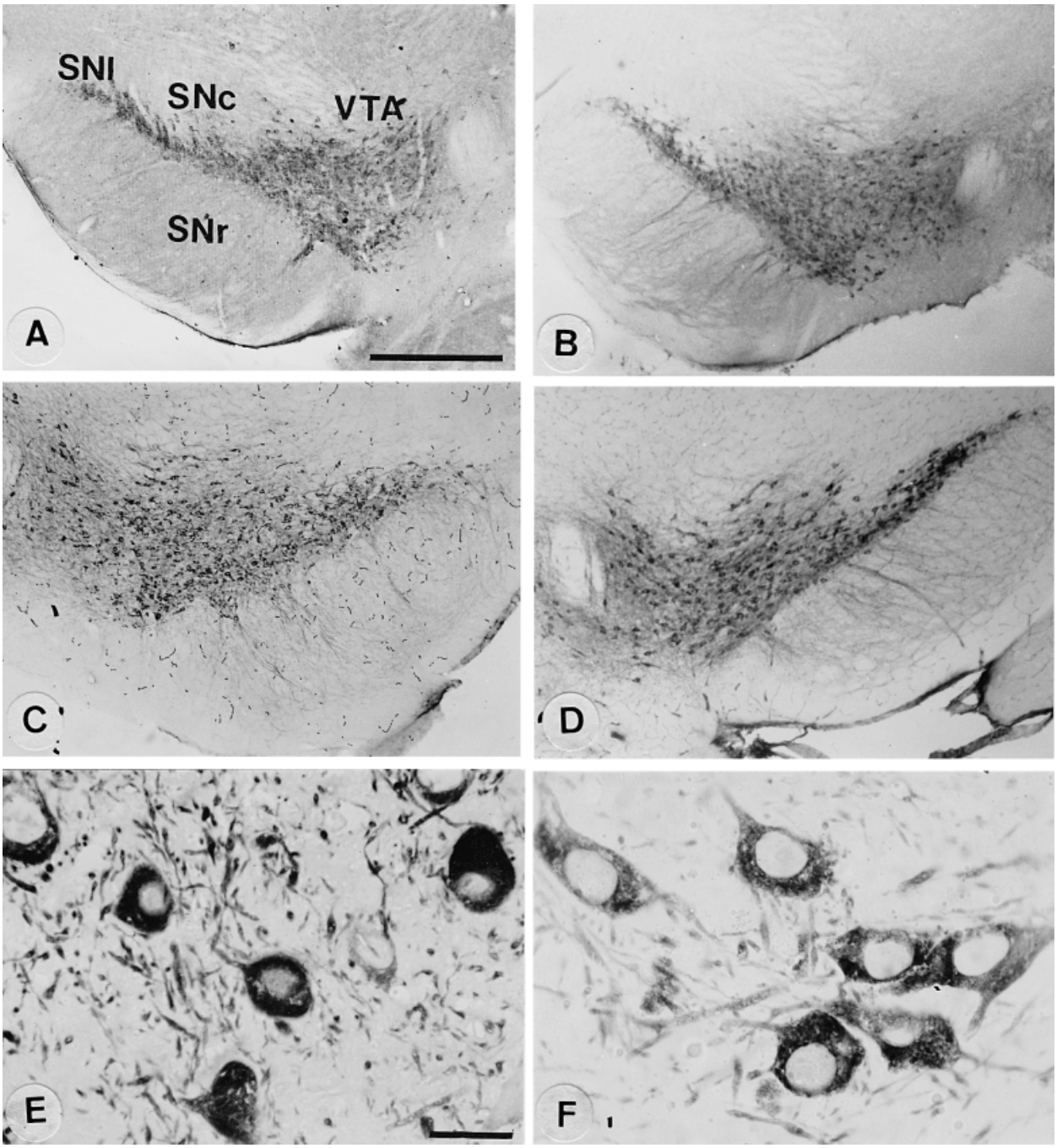

FIG.1. Immunohistochemical detection of TH and DDC at the light microscopic level in the midbrain. (A, C and E) $DAT^{+/+}$ mice. (B, D and E) $DAT^{-/-}$ mice. DDC (A and B) and TH (C and D) immunohistochemistry in the ventral midbrain following Vibratome 60 µm sections. (E and F) TH immunohistochemistry on 1-µm semi-thin sections. Note that the number, morphology and distribution of dopaminergic neurons are not affected by inactivation of the dopamine transporter gene. A slight reduction in the intensity of the immunohistochemical signal is observed on semi-thin sections, which correlates with the results of Western blotting (see below). Scale bar, 500 µm (A–D); 20 µm (E and F).

1999), that we have previously described. Thus, we investigated the expression and regulation of TH in these animals using different approaches to determine levels of mRNA and protein, along with TH distribution at the regional, cellular and subcellular level. Our results demonstrate that the nigrostriatal dopamine system is relatively intact and reveal that the regulation of TH *in vivo* is multifaceted, highlighting the central role of this enzyme and its regulatory mechanism of compensation to alteration in dopaminergic transmission.

Materials and methods

Animals

The DAT mutant mice were generated as previously described (Giros *et al*., 1996). Both the wild-type ($DAT^{+/+}$) and mutant mice ($DAT^{-/-}$) were bred and kept in standard housing conditions in the transgenic animal facility at the University of Bordeaux II Victor Segalen. Because $DAT^{-/-}$ females fail to care for their offspring, $DAT^{+/+}$ and $DAT^{-/-}$ mice were obtained by crossing heterozygotes ($DAT^{+/-}$), and

TABLE 1. Numbers of TH cell bodies in the SNc and VTA with *in situ* hybridization (ISH) and immunohistochemistry (IHC)

	TH cell bodies (ISH)		DDC cell bodies (ISH)		TH cell bodies (IHC)		DDC cell bodies (IHC)	
	SNc	VTA	SNc	VTA	SNc	VTA	SNc	VTA
$DAT^{+/+}$	112 ± 7	192 ± 17	109 ± 12	187 ± 15	121 ± 15	227 ± 21	127 ± 17	216 ± 19
$DAT^{-/-}$	88 ± 8**	153 ± 14*	82 ± 11**	147 ± 17**	87 ± 19**	181 ± 19*	81 ± 26*	178 ± 17*

*$P < 0.05$; **$P < 0.01$. Two-tailed Student's *t*-test.

TABLE 2. mRNA and protein levels of dopamine system markers in the SNc, VTA and striatum: *in situ* hybridization (ISH), Western blot and binding

	TH mRNA in VMB (ISH)		DDC mRNA in VMB (ISH)		TH protein (Western blot)		DDC protein (Western blot)		VMAT protein (binding)
	Macro	Micro	Macro	Micro	VMB	Striatum	VMB	Striatum	Striatum
$DAT^{+/+}$ (%)	100	100	100	100	100	100	100	100	100
$DAT^{-/-}$ (%)	97	68**	102	70*	66**	12***	107	92	71.27**

mRNA levels for TH and DDC were quantified using *in situ* hybridization (ISH) at the macro- and microautoradiographic level. protein levels for TH and DDCwere quantified using Western blot, and using macroautoradiographic binding for the VMAT. Statistical analyses were performed on raw data (see Materials and methods for details), then control values (for $DAT^{+/+}$ animals) were set to 100 and $DAT^{-/-}$ values were expressed relative to them.
$P < 0.05$; **$P < 0.01$; ***$P < 0.001$, two-tailed Student's *t*-test.

offspring were genotyped by Southern blot analysis of DNA extracted from tail biopsies. Up to 35% of $DAT^{-/-}$ mice died before adulthood as previously reported (Giros *et al*., 1996), and thus < 15% of the genotyped offspring that reached adulthood were $DAT^{-/-}$. Housing of the animals and all experimental procedures are in accordance with the guidelines of the French Agriculture and Forestry Ministry (decree 87849, license 01499).

In situ *hybridization*

Mice were anaesthetized with chloral hydrate and perfused transcardially with 1% paraformaldehyde in phosphate-buffered saline (PBS). The brains were removed, immersed in the same fixative for 1 h and then cryoprotected overnight at 4 °C in 15% sucrose. The brains were then frozen over liquid nitrogen, cut into 12-µm frontal sections, mounted on slides coated with gelatin, and stored at –80 °C until use. The *in situ* hybridization procedure was performed as previously described (Jaber *et al*., 1995) with oligonucleotide probes designed to recognize the mRNA of either DAT (Giros *et al*., 1991), DOPA decarboxylase (DDC) (Tanaka *et al*., 1989), TH (Grima *et al*., 1985) or D_2 receptor (Giros *et al*., 1989). The probes were labelled by tailing with [^{35}S]dATP (NEN) to a specific activity of 2×10^9 cpm/µg. Sections were thawed, incubated for 1 h in the prehybridization buffer, rinsed in 4 × SSC, then acetylated, dehydrated in absolute ethanol, and dried at room temperature. Following this procedure, the slides were incubated at 42 °C overnight with probes at a concentration of 5 ng/µL in the hybridization solution. The next day, they were washed in decreasing concentrations of SSC for 3 h and were dehydrated in ethanol. Slides were exposed at room temperature to X-ray (X-R) film (Kodak X-Omat) for 5 days for the detection of TH, DAT and DDC mRNA, and 7 days for that of the D_2 receptors mRNA. The quantification procedure was performed with a Biocom 200 image analyser (Les Ulis, France). For macroautoradiographic analysis, the optic density (OD) of the standards was measured, and the calibration curve representing OD as a function of the radioactivity concentration was obtained. Probe concentration and exposure times were chosen in order to stay within linear range of the film. For anatomical visualization and microautoradiographic analysis, sections were then dipped into Amersham's LM-1 liquid emulsion diluted 1/3 in water, exposed in the dark for 6 weeks, then developed and counterstained with haematoxylin. Grain counting at × 50 magnification was used and neurons that showed a grain density superior to the background were considered as positive cells. The mean background value was subtracted from the grain density measured on each cell. The final data were converted into quantity of radioactivity using a calibration curve constructed with the brain paste standards. Samples from individual animals were always analysed in duplicate or triplicate. Comparisons were made between groups of animals ($n = 6$) using the Student's *t*-test. Results were expressed as percentage relative to control values.

Immunohistochemistry

Mice were anaesthetized with chloral hydrate and perfused through the heart with 10–20 mL of 0.9% NaCl and 100 mL of 2% paraformaldehyde in 0.1 M phosphate buffer, pH 7.4, alone or with 0.1% glutaraldehyde for electron microscopy. Brains were removed, stored overnight in 2% paraformaldehyde in 0.1 M phosphate buffer, pH 7.4, and cut into 60-µm frontal sections using a Vibratome. The sections were cryoprotected in PBS solution containing 30% sucrose and freeze-thawed in isopentane to improve penetration of immunoreagents. The sections were then pre-incubated for 1 h at RT in PBS with 0.2% BSAc (acetylated and partly linearized bovine serum albumin from Aurion, The Netherlands), before processing for immunohistochemistry. DDC (kind gift from Dr Krieger) (Krieger *et al*., 1993) and serotonin (kind gift from Dr D. Fellmann) (Bugnon *et al*., 1983) antibodies were raised in rabbit. TH immunoreactivity was used as a marker of dopaminergic neurons in mesencephalic sections (Fig. 1C–F) and was detected with a monoclonal antibody (Incstar, USA). The same animals from each genotype ($DAT^{+/+}$ $n = 8$ and $DAT^{-/-}$ $n = 6$) were analysed using both immunoperoxidase and immunogold techniques. Samples from individual animals were always analysed in duplicate or triplicate.

Immunoperoxidase technique

Sections were incubated with the TH or DDC antibodies diluted at 1/5000 in PBS–BSAc for 48 h at 4 °C. Following three washes in PBS, TH sections were then incubated with a goat anti-mouse biotinylated antibody, serotonin and DDC sections with a goat anti-rabbit

biotinylated antibody (Amersham, UK) at a dilution of 1/200 for 1 h at RT. Sections were then washed in PBS and incubated with the ABC complex (0.5% in PBS) (ABC, Vectastain-Elite, Vector Laboratories, USA) for 1 h at RT. TH and DDC immunoreactivity were visualized by incubation in H_2O_2-diaminobenzidine nickel ammonium sulphate (DAB) solution as previously described (Jaber

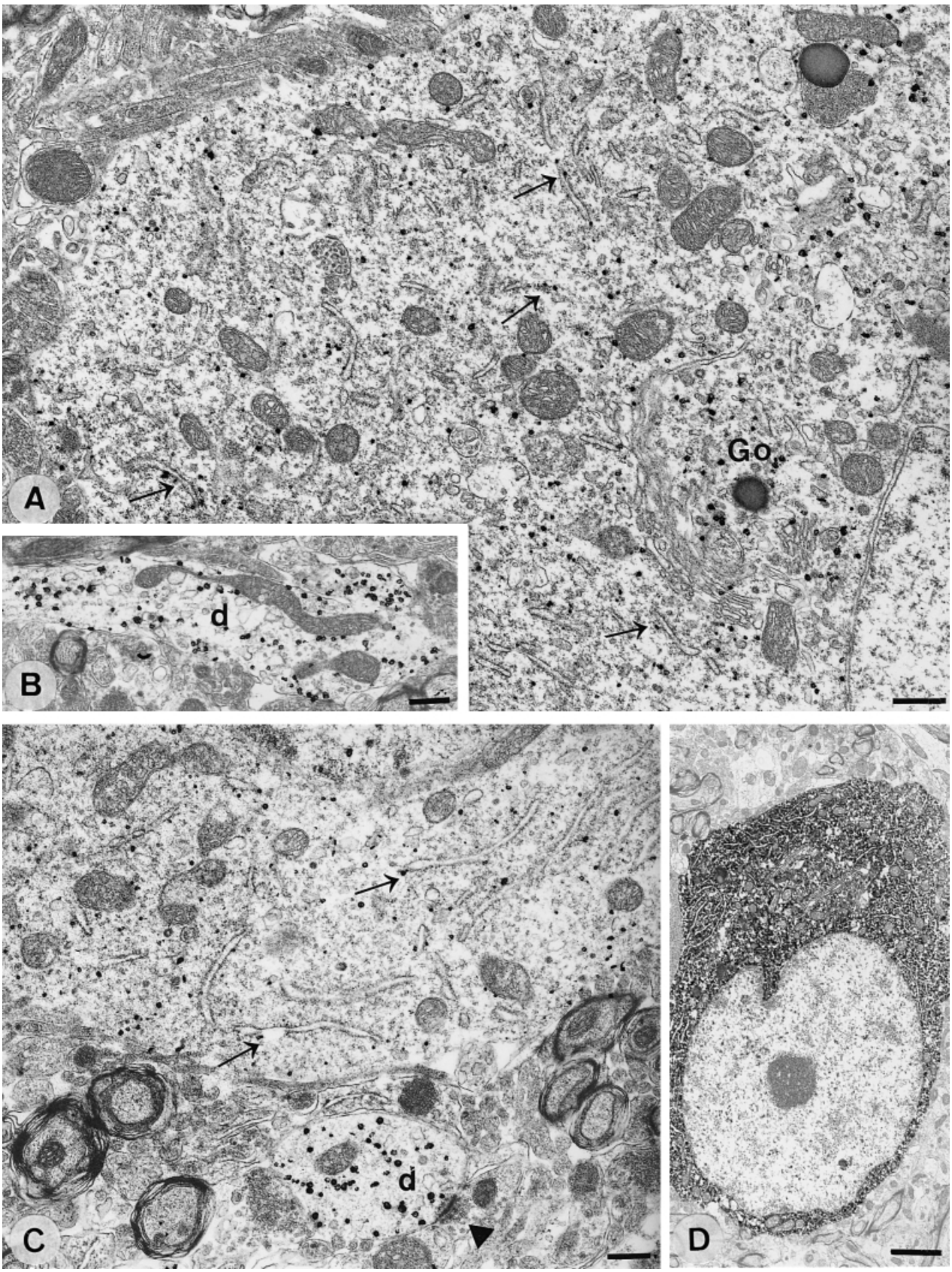

et al., 1995). For TH electron microscopy detection, areas of interest, the substantia nigra (SN) compacta and dorsal striatum, were postfixed in osmium tetroxide for 30 min, then were washed in PBS and dehydrated in a graded series of dilution of ethanol and propylene oxide. Sections were then preimpregnated with a 1 : 1 mixture of Araldite and propylene oxide for 1 h, impregnated with Araldite overnight and then flat-embedded in Araldite. Semi-thin sections (1 µm) were cut with a Reichert Ultracut S (Leica), collected on glass slides, dried and mounted.

Immunogold technique

The sections were incubated in TH antibody as described for the immunoperoxidase procedure. After washing twice in PBS–BSAc and twice in PBS–BSAc supplemented with 0.1% fish gelatin (Aurion) (PBS–BSAc–gelatin), sections were then incubated for 24 h at RT in goat anti-mouse IgG conjugated to ultra small colloidal gold (0.8 nm, Aurion) diluted in PBS–BSAc–gelatin (1 : 50). The immunogold signal was intensified using a silver enhancement kit (Aurion). The reaction was carried out in the dark at RT and stopped by two washes in 2% sodium acetate. The signal was then amplified by immersion of the sections in gold chloride (0.05%) and then in sodium thiosulphate (0.3%) for 2×10 min at 4 °C. Serial ultrathin sections of immunogold-treated material were cut with a Reichert ultracut S (Leica). They were collected on copper grids, contrasted with uranyl acetate and lead citrate, and observed with a Philips CM10 electron microscope.

Quantification of TH immunoreactivity following electron microscopy analysis

Levels of TH were measured at the ultrastructural level by using plates of immunolabelled cell bodies and dendritic shafts. Morphometric analysis was performed on photo negatives by using Metamorph software (Universal Imaging, Paris, France). The measures were performed in sections from $DAT^{+/+}$ and $DAT^{-/-}$ mice ($n = 3$; with an average of 10 cell bodies and 10 dendrites analysed for each animal). Gold immunoparticles above background levels were counted and the results were expressed as the number of immunoparticles per μm^2 in dendrites and cell bodies.

Western blots

Frozen tissues from $DAT^{+/+}$ and $DAT^{-/-}$ were sonicated for 10 s in 500 µL of sodium dodecyl sulphate (SDS) 2%, Tris 20 mM pH 8, EDTA 5 mM. Extracts were then heated for 5 min at 90 °C and centrifuged at 13 000 r.p.m. for 15 min. Total protein in the supernatants was quantified using the Biorad Dc protein assay. Thirty micrograms of proteins was used for electrophoresis on 12% SDS–polyacrylamide gels and transferred to nitrocellulose. TH and DDC antibodies were used at a dilution of 1/10 000 and 1/5000, respectively. Immunoreactivity was detected with horseradish-peroxidase (HRP)-labelled antibodies followed by chemiluminescent detection (ECL kit from Amersham). Autoradiographic densitometry was performed with a Biocom 200 image analyser (Les Ulis). A standard curve was obtained with various amounts of protein extracts from striatum ranging from 0 to 20 µg. The ODs of the standards were measured, and a calibration curve representing OD as a function of the protein concentration was calculated. Samples from individual animals were always analysed in duplicate or triplicate. Comparisons were made between groups of animals ($n = 6$) using the Student's *t*-test. Results were expressed as percentage relative to control.

Monoamines vesicular transporter binding

In vitro autoradiographic detection and quantification of monoamines vesicular transporter (VMAT) were performed following [^{3}H]TBZOH [dihydrotetrabenazine (2-hydroxy-3-isobutyl-9,10-dimethoxy-1,2,3,4,6,7-hexahydro-11b(H)benzo[α]quinolizine] binding to mice brain slices as previously described (Darchen *et al*., 1989). In summary, 20-µm sections of frozen $DAT^{+/+}$ or $DAT^{-/-}$ brain were pre-incubated for 5 min at room temperature in 0.3 M sucrose and 20 mM HEPES (*N*-2-hydroxyethylpiperazine-*N*-1-2-ethane sulphuric acid) at pH 8.0. Incubation proceeded for 1 h 45 min in the same sucrose medium supplemented with 0.125 nM [^{3}H]TBZOH (Amersham). Non-specific binding was estimated from adjacent sections in the same solution supplemented with 1 µM tetrabenazine. After two × 3 min washes in Tris(HCl) 50 mM, pH 8.0 at 4 °C and a 2 s rinse in ice-cold distilled water, slices were air dried and exposed for 2 weeks to [^{3}H]Hyperfilm (Amersham). Optical density on the autoradiographic film was measured using a Biocom image analyser and converted to fmol [^{3}H]TBZOH specifically bound per mg tissue compared with [^{3}H]-labelled standards (Amersham). The non-specific binding on the control slices was not distinguishable from the background of the autoradiographic film.

Results

Dopamine neurons of the ventral midbrain

DDC- and TH-immunoreactive neurons were present mainly in the ventral tegmental area (VTA) and the three subdivisions of the SN (pars compacta, pars lateralis and pars reticulata, Fig. 1). Processes emerging from TH-positive neurons were found to spread normally throughout the whole pars reticulata in $DAT^{+/+}$ and $DAT^{-/-}$ mice (Fig. 1C and D). The general morphology of DDC- and TH-positive neurons was identical in $DAT^{+/+}$ and $DAT^{-/-}$ mice (Fig. 1). All DDC- and TH-positive neurons were counted at Bregma-2,9 to –3,2 (Franklin & Paxinos, 1997, Fig. 1). As summarized in Table 1, a slight decrease was found in the number of DDC- (24.7 ± 6.1%) and TH- (27.6 ± 4.5%) labelled neurons in both the SNc and the VTA.

At the electron microscopic level, the TH-immunoreactive perikaryon and dendrites in the SNc, visualized using both immunogold (Fig. 2A–C) and immunoperoxidase (Fig. 2D) procedures, showed large distribution of the staining in both $DAT^{+/+}$ (Fig. 2A and B) and $DAT^{-/-}$ (Fig. 2C and D) mice. In the perikaryon of $DAT^{-/-}$ mice, the DAB reaction product is homogeneous and diffuses over the entire cytoplasm (Fig. 2D). In both $DAT^{+/+}$ and $DAT^{-/-}$ mice, the gold particles were mainly associated with the Golgi apparatus cisternae and the cytoplasmic faces of the endoplasmic reticulum (Fig. 2A and C). In the immunoreactive dendrites (Fig. 2B and C), the gold particles were randomly distributed throughout the cytoplasm. Quantification of the number of gold particles/μm^2

FIG. 2. Immunohistochemical detection of TH at the electron microscopic level in the substantia nigra. (A and B) $DAT^{+/+}$ mice. (C and D) $DAT^{-/-}$ mice. (A) A TH-immunoreactive perikaryon shows a large distribution of immunogold particles in the cytoplasm that are mainly associated with Golgi apparatus (Go) and the cytoplasmic face of the endoplasmic reticulum (arrowheads). (B) TH-positive dendrite (d) with a homogeneous distribution of immunogold particles. (C) TH immunoreactivity is slightly reduced in the perikaryon but is present at normal levels in dendrites (d); arrowhead points to a symmetrical synaptic contact between a TH-immunoreactive dendrite and a terminal. (D) Low-power electron micrograph of TH-positive perikaryon (immunoperoxidase labelling) showing a round unindented nucleus; note the homogeneous distribution of TH over the entire cytoplasm. Scale bar, 0.5 µm (A–C); 20 µm (D).

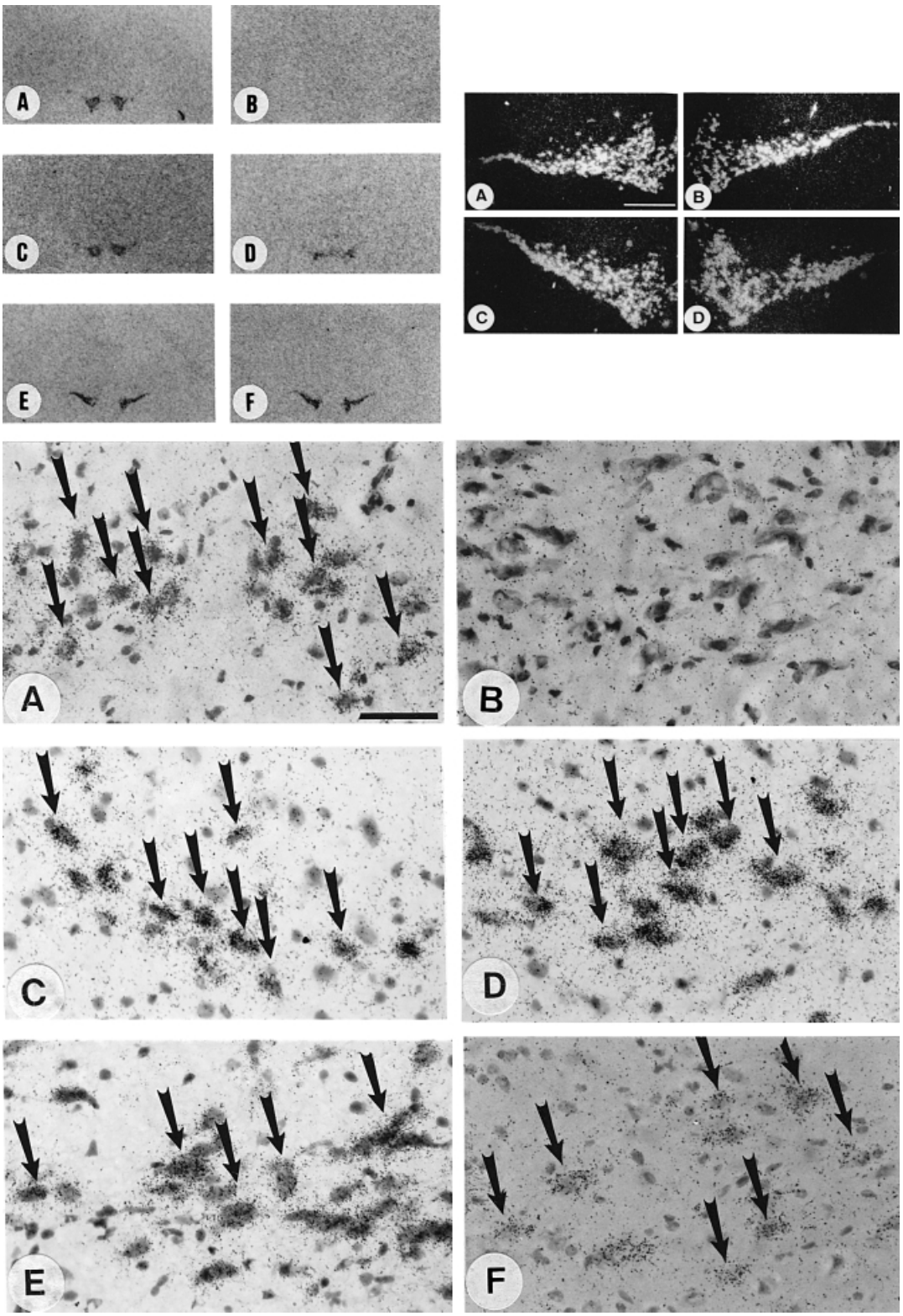

FIG. 3. *In situ* hybridization of DAT, D2, DDC and TH mRNA in the ventral midbrain of wild-type and homozygote mice. (Upper left panel) Macroautoradiography following *in situ* hybridization with DAT (A and B), D2 (C and D) and TH (E and F) oligonucleotide probes. DAT mRNA is not expressed in $DAT^{-/-}$ (B) while D2 autoreceptors mRNA were reduced (C and D) and TH mRNA showed no modification. (Upper right panel) Dark-field microscopy following microautoradiography showing no modification in the number of labelled neurons or the intensity of labeling of TH (A and B) and DDC (C and D) mRNAs in the ventral midbrain of $DAT^{-/-}$ mice. (Lower panel) Light-field microscopy following microautoradiography with probes against mRNA for the DAT (A and B), D2 (C and D) and TH (E and F) mRNAs showing specific cellular labelling with each probe (see arrows). Dopamine cells of the SNc of $DAT^{-/-}$ mice do not express the DAT mRNA. The number of cells expressing TH mRNA is slightly reduced in $DAT^{-/-}$ mice.

showed no modification in dendrites (8.27 ± 2.12 and 12.5 ± 3.7 gold particles/μm^2) and a significant decrease (39%) in the perikaryon (10.06 ± 1.63 and 6.5 ± 0.41 gold particles/μm^2) of the TH-positive neurons of $DAT^{+/+}$ and $DAT^{-/-}$, respectively.

TH mRNA levels in the ventral midbrain

Macroautoradiographic analysis of X-R films following quantitative *in situ* hybridization was performed in the ventral midbrain, comprising the SNc and the VTA, and provided an overall view of the localization of DAT and TH demonstrating a homogeneous labelling of these mRNA. Our results revealed a lack of DAT mRNA and a decrease in D2 autoreceptor mRNA (–42.8 ± 9%; $P < 0.01$, Fig. 3, upper left panel) in $DAT^{-/-}$ mice as described previously (Giros *et al*., 1996). No significant modifications in the levels of either TH or DDC mRNAs were found, although there was a tendency towards a decrease in $DAT^{-/-}$ mice (Table 1). Because of the limited resolution provided by X-ray films and the small areas analysed, slight modifications of the mRNA levels can not be detected. Thus, we performed quantification at the cellular level of the corresponding mRNAs (Fig. 3, upper left panel). All TH mRNA-positive neurons were counted at the same coordinates as for immunohistochemistry (Fig. 3, lower panel). As shown in Table 1, there was a decrease in the number of TH- (–31.4 ± 7.2%) and DDC- (–29.8 ± 6.9%) labelled cells in accordance with our immunohistochemistry results. Furthermore, we found a significant decrease in the overall labelling for TH (–24.1 ± 6.2%) and DDC (–27.8 ± 8.7%) mRNAs in the ventral midbrain that was of the same order of magnitude as the percentage of cell loss. However, we found no significant modification in the grain density per cell expressing either TH or DDC mRNA. Thus, the decrease in mRNA levels of TH and DDC is due to the decrease in the number of dopamine cells.

TH, DDC and VMAT protein levels in the basal ganglia

Results obtained regarding the number of TH and DDC cells as well as the corresponding mRNA levels in the ventral midbrain do not account for the dramatic decrease of intracellular dopamine levels in the striatum that we previously described (Jones *et al*., 1998). Quantification of TH protein levels in the ventral midbrain, striatum and adrenal (used as control) were assessed using Western blotting (Fig. 4). The levels of TH protein were found to be decreased by 90% in the striatum of $DAT^{-/-}$ mice and by only 35% in the ventral midbrain (VMB). The per cent decrease in TH protein levels in the midbrain is in accordance with TH mRNA levels and the number of TH-positive cells (Fig. 4). However, the discrepancy in the levels of TH protein in striatum versus midbrain may suggest either a trafficking dysfunction, a differential regulation of TH in the cell bodies of dopamine neurons in the ventral midbrain compared with their terminals in the striatum, or loss of striatal projections. In order to investigate this issue, we performed DDC Western blotting on the same samples and found that DDC protein levels were not modified in all tissues investigated (Fig. 4). These data, along with the *in situ* hybridization results, strongly suggest that the extensive loss of TH proteins in the striatum is not due to loss of dopamine neurons or projections.

Furthermore, we performed quantitative macroautoradiographic analysis following binding of [^{125}I]aminoiodoketanserin to VMAT, highly expressed in dopaminergic terminals. Surprisingly, levels of VMAT were found to be 23.3 ± 1.6 pmol/mg tissue ($n = 4$) in $DAT^{+/+}$ animals and 16.6 ± 1 pmol/mg tissue ($n = 4$) in $DAT^{-/-}$. Thus, VMAT decreased by 28.75% in $DAT^{-/-}$, a percentage which is of the same order of magnitude as the dopaminergic cell loss (Table 1, Fig. 6). Thus, the absence of modifications in DDC expression may be related to the fact that low modifications are covered by the non-neuronal expression of DDC, e.g. in blood vessels. However, as we will discuss

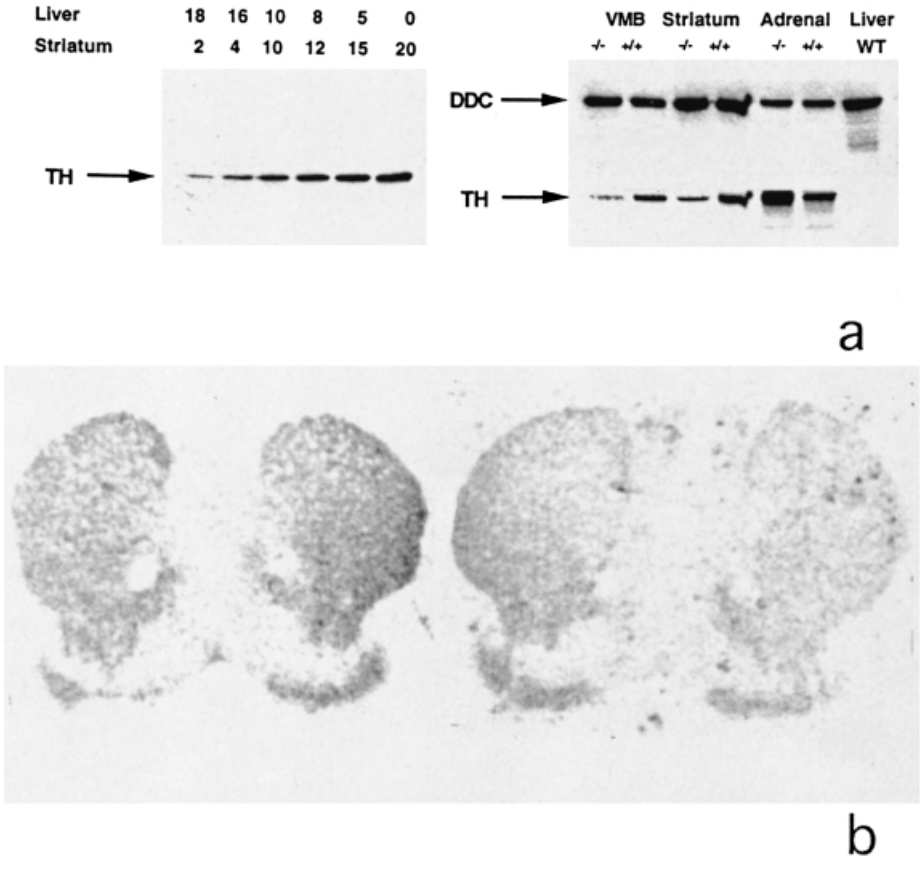

FIG. 4. Quantification of TH, DDC and VMAT protein levels in wild-type and homozygote animals. (a) Western blot on protein extracts from ventral midbrain, striatum, adrenal and liver of $DAT^{+/+}$ and $DAT^{-/-}$ mice. A standard curve was obtained with various amounts of protein extracts from striatum ranging from 0 to 20 µg. Liver protein extracts, known not to contain TH, ranging from 20 to 0 µg were added to the gel wells in order to always transfer the same amount of protein. Quantification of the signal intensity revealed a 90% decrease of TH protein levels in the striatum and 35% decrease in the ventral midbrain of $DAT^{-/-}$ compared with $DAT^{+/+}$. DDC protein levels were not modified as demonstrated by Western blotting of the same samples with DDC antibody following removal of the TH antibody using standard procedures (see Materials and methods). (b) Autoradiographic binding of VMAT at the striatal level of $DAT^{+/+}$ (left) and $DAT^{-/-}$ (right) mice. Note the reduction in the OD in $DAT^{-/-}$ animals.

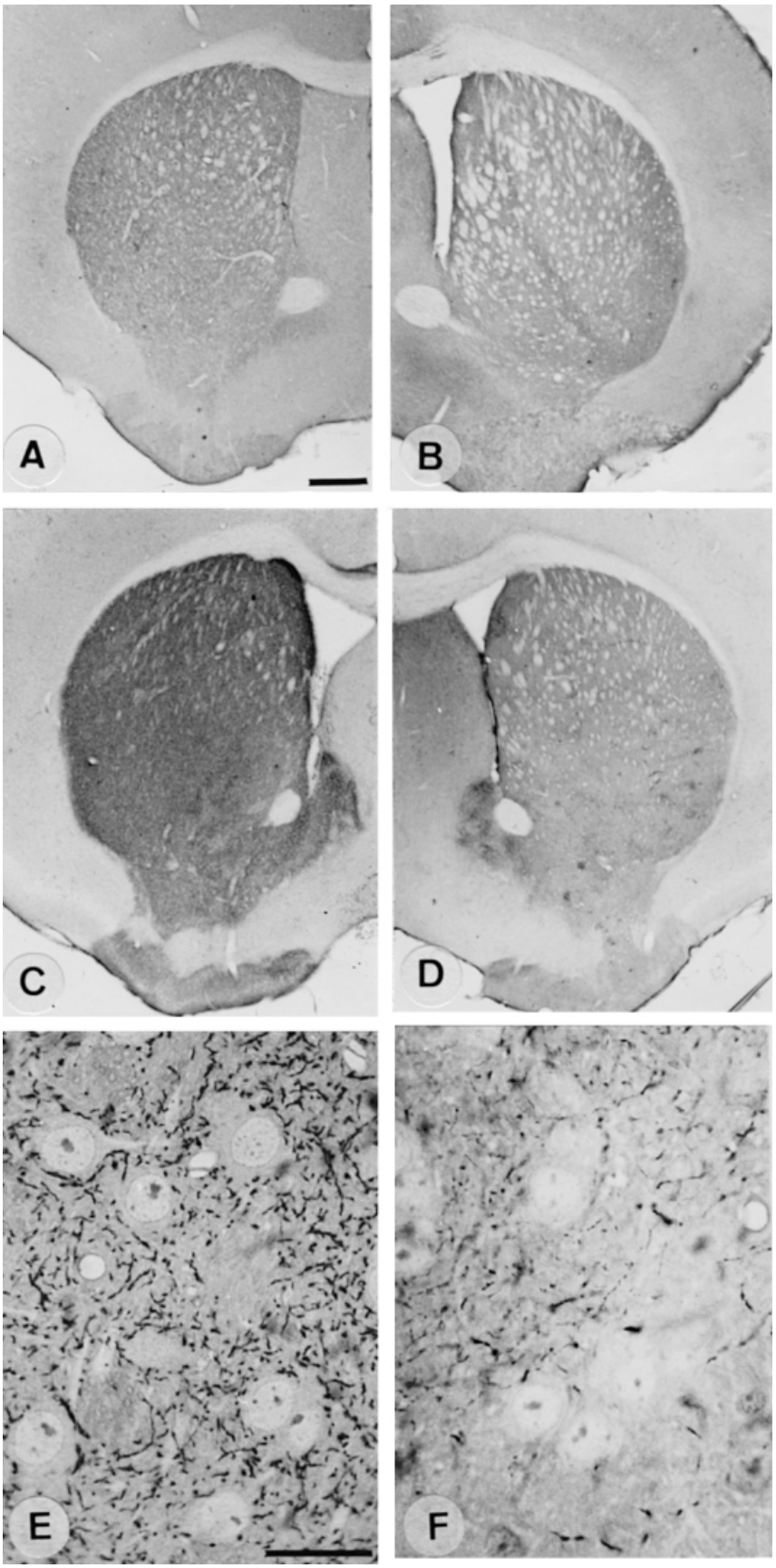

FIG. 5. Immunohistochemical detection of TH and DDC at the light microscopic level in the striatum. (A, C and E) $DAT^{+/+}$ mice. (B, D and F) $DAT^{-/-}$ mice. DDC (A and B) and TH (C and D) immunohistochemistry following Vibratome 60 µm sections. (E and F) TH immunohistochemistry on 1-µm semi-thin sections. Note that TH immunoreactivity, but not DDC, is significantly reduced in the striatum. This decrease is heterogeneous as the accumbens is labelled more than the dorsal striatum. This heterogeneity is also observed in the dorsal striatum as revealed on semi-thin sections. Indeed, while TH distribution in $DAT^{+/+}$ wild-type is widespread and homogeneous, the striatum of $DAT^{-/-}$ animals presents regions with no detectable labelling and a few others with nearly normal labelling (see also Fig. 6). Scale bar, 500 µm (A–D); 20 µm (E and F).

below, neither DDC nor VMAT labelling can be attributed to serotonin or noradrenaline projections to the striatum.

Heterogeneous and specific reduction of TH labelling in the striatum

In order to investigate the cellular mechanisms underlying the dramatic loss of TH protein levels in the striatum compared with the ventral midbrain, we performed striatal immunohistochemical detection of TH at the light (Fig. 5) and electron microscopy level (Fig. 6). The distribution of TH was apparently heterogeneous at both the anatomical and cellular levels in $DAT^{-/-}$ mice. As seen in Fig. 5, TH labelling is markedly decreased in the striatum as demonstrated on 60-μm Vibratome sections. Moreover, this decrease is heterogeneous as it is less pronounced in the core and shell of the nucleus accumbens, as well as in the olfactory tubercle, than in the dorsal part of the striatum. No modification in either DDC expression or distribution was observed (Fig. 5), in correlation with the Western blot results, and again pointing to the anatomical integrity of the dopaminergic terminals in the striatum. In order to investigate the participation of serotonin projections to the expression of DDC and VMAT we performed serotonin immunohistochemistry in the striatum and found very rare and scarce labelling of serotonin (data not shown) in both $DAT^{+/+}$ and $DAT^{-/-}$ mice that can not account for widespread expression of either DDC (Fig. 5) or VMAT (Fig. 4). Moreover, immunohistochemistry with a dopamine β hydroxylase antibody, a marker of the locus coeruleus noradrenergic cell bodies and projections, was used in order to investigate whether the remaining TH labelling might be due to noradrenergic projections from the locus coeruleus. This antibody clearly labelled neurons of the locus coeruleus but gave only an extremely faint labelling in the ventral part of the shell of the accumbens and no labelling in the dorsal striatum (data not shown).

In mice lacking the DAT, semi-thin sections (1 μm) showed that, even within a given region (i.e. the dorsal striatum), TH labelling was decreased in a heterogeneous manner (Fig. 6). $DAT^{+/+}$ mice showed a dense network of TH-immunoreactive fibres in the striatal neuropil (Fig. 6), while $DAT^{-/-}$ mice displayed a more restricted distribution with areas almost empty of any labelling while few areas still showed some TH immunoreactivity. These findings were especially striking when investigated at the electron microscopy level. Indeed, while most of the dorsal striatum is lacking any TH labelling in $DAT^{-/-}$ as compared with $DAT^{+/+}$, few remaining TH-immunoreactive profiles can still be observed and are in fact indistinguishable from $DAT^{+/+}$ TH profile (see also legend of Fig. 6). In both $DAT^{-/-}$ and $DAT^{+/+}$ the ultrastructural characteristics of the TH labelling were the same (Fig. 6). The immunostained structures exhibited varicosities while the enlarged profiles were filled with mitochondria. Nearly all of the profiles, irrespective of their size, contained vesicles. In the striatum, many features previously described for TH projections were observed. Indeed, close inspection of the images revealed the existence of separate populations of small clear vesicles and large dense core vesicles that can be found in the same terminals (Fig. 6). The large dense core vesicles always outnumbered the smaller clear vesicles and rarely occurred next to the synaptic junction (Fig. 6B and C), as previously described (Wassef *et al*., 1981; Freund *et al*., 1984; Matteoli *et al*., 1991; Pickel *et al*., 1996). Moreover, we found that the most common postsynaptic targets of tyrosine hydroxylase-immunoreactive boutons were dendritic spines and shafts, and that the large majority of the synaptic contacts identified formed symmetric junctions onto dendritic shafts and spines (Fig. 6D). Such symmetrical synapses are characterized by a narrow postsynaptic density and by a synaptic cleft less enlarged than a normal membrane opposition. However, rare asymmetric synapses were found between a TH-immunoreactive profile and dendritic spines (Fig. 6B).

TH-positive neurons in the striatum

While investigating the distribution of TH immunoreactivity in the striatum of $DAT^{-/-}$ mice, we observed the presence of TH-immunoreactive neurons (Fig. 7). These neurons were visualized on 60-μm Vibratome sections, on 1-μm semi-thin sections, as well as by electron microscopy following either peroxidase or immunogold staining. The TH-immunoreactive perikaryon fulfil the structural features of dopaminergic neurons as well as those of striatal interneurons in general. The peroxidase reaction was observed over the entire cytoplasm with a distribution of TH labelling as observed in dopaminergic neurons of the SN in Fig. 2D. The number of neurons varied greatly within animals, with some animals having over 80 neurons per hemi-striatum. These neurons were medium sized, as opposed to large-sized cholinergic neurons, and were present more in the ventral than dorsal striatum (Fig. 7A and B). No such neurons were visible in the striatum of $DAT^{+/+}$ animals, which is most probably due to the extensive labelling of TH projections from the midbrain that may cover the weak labelling of striatal TH cell bodies when using immunohistochemistry. However, *in situ* hybridization revealed the existence of TH mRNA not only in $DAT^{-/-}$ striatal sections but also in $DAT^{+/+}$ animals (Fig. 7). The number of TH mRNA-positive neurons per hemi-striatum was 35 ± 19 in $DAT^{-/-}$ and 21 ± 12 in $DAT^{+/+}$, and was not statistically different although there was a tendency towards an increase in $DAT^{-/-}$. Differences between the number of neurons found using immunohistochemistry and *in situ* hybridization are probably due to the difference in the thickness of sections (60 μm versus 12 μm). In addition, the expression of TH mRNA was very faint and slides needed to be exposed for 3 months for the signal to be detected. In comparison, TH mRNA in the SN is visualized within 3 weeks of exposure.

Discussion

In this work, we examined the neuroanatomy of dopamine neurons, and projections in mice lacking the DAT in the nigrostriatal and mesolimbic pathway. The main findings presented here can be summarized as follows. (i) The extensive decrease in the levels of TH and dopamine are not due to loss of either dopamine neurons or projections. (ii) While TH mRNA levels in the VMB were only slightly decreased, protein levels were decreased by 90% in the striatum. (iii) Within the dorsal striatum, TH immunoreactivity is almost absent except in a few projections that maintain normal labelling and morphology. (iv) Finally, TH-positive neurons were observed in the striatum of $DAT^{-/-}$ and, to some extent, in $DAT^{+/+}$ animals. These neurons, along with the few remaining TH projections, may be promoting the dopaminergic volume transmission that we previously proposed in this animal model (Jones *et al*., 1998). These results suggest that while the morphology and anatomical integrity of the nigrostriatal pathway appear relatively intact in $DAT^{-/-}$ animals, the adaptive changes in response to the lack of DAT in various parameters of the TH system that we found here and in other parameters of the DA transmission (Giros *et al*., 1996; Jones *et al*., 1998) are of a magnitude and number not encountered previously in a single system. Thus, along with our previous findings, these results demonstrate, *in vivo*, that mRNA, protein, activity and distribution of TH can be independently regulated to an extent that has not been yet appreciated. In addition, they point to the DAT as the major regulatory element controlling the dopaminergic transmission as its inactivation can not be compensated by any of the dramatic changes in DA homeostasis that we described here and before (Giros *et al*., 1996; Jones *et al*., 1998).

Few reports have previously shown a dissociation between TH mRNA and protein levels. For instance, Pasinetti *et al*. (1992) have described that in an animal model where dopamine neurons were lesioned by 6-OHDA, TH protein levels are relatively increased in the

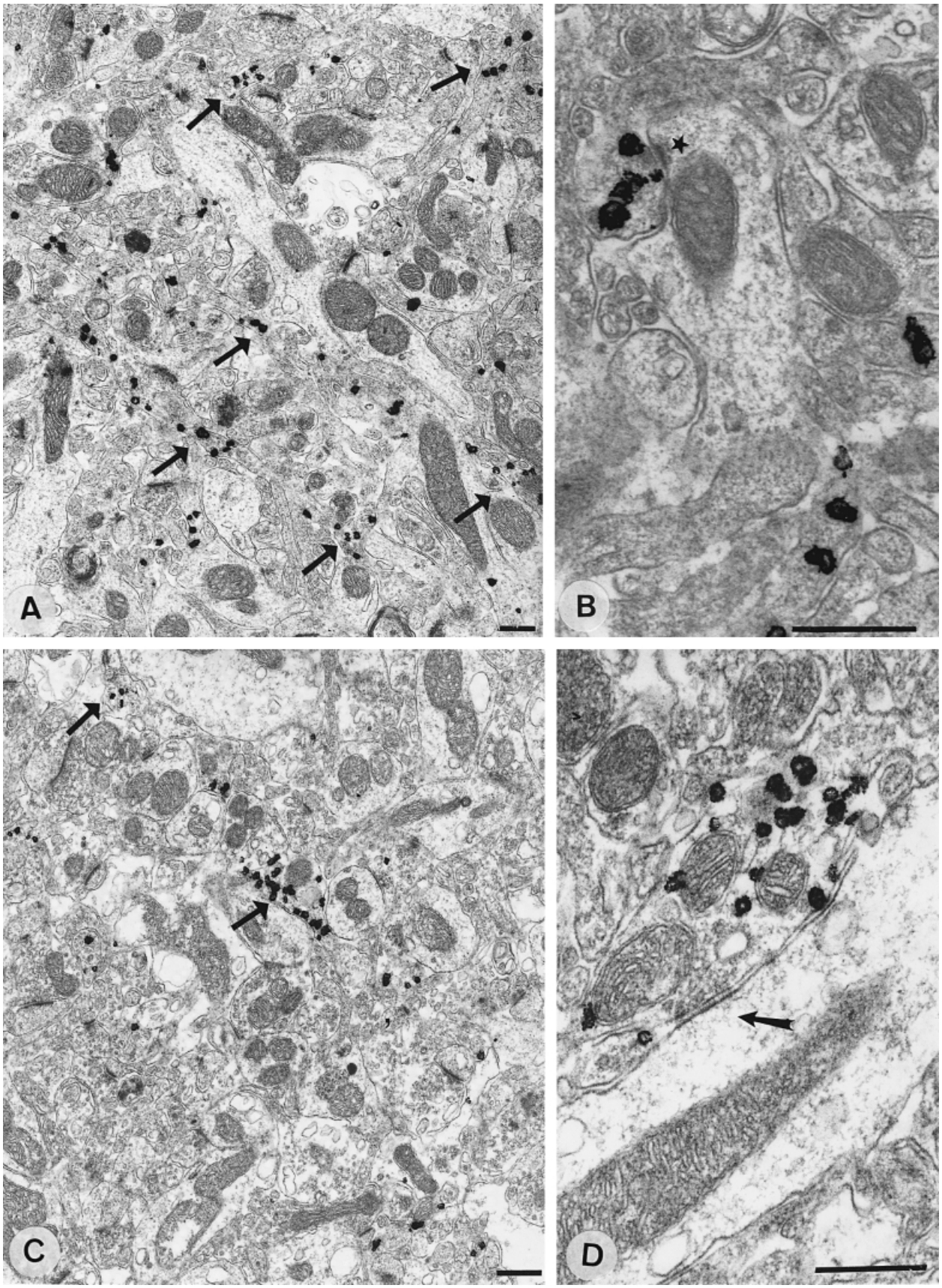

remaining few neurons while TH mRNA is decreased. Here we show a dissociation between TH mRNA and protein, where mRNA level is decreased by 25% and protein levels are decreased by 90%. The results presented here, along with an increasing number of examples (Kaneda *et al*., 1991; Kumer & Vrana, 1996), indicate that levels of TH mRNA do not necessarily correspond to levels of TH protein or activity in contrast to other dopaminergic markers, e.g. the dopamine receptors (Jaber *et al*., 1996).

TH immunohistochemistry and Western blots studies on $DAT^{-/-}$ animals have shown a significant and specific decrease of labelling in the dorsal striatum, a lesser decrease of TH in the ventral striatum (shell and core of accumbens, olfactory tubercle) and the VMB (SNc and VTA). This demonstrates that with the same mRNA levels, TH can be differentially regulated at the protein levels in relation to the area of projection. The molecular basis of this decrease is currently under investigation. One possible clue may lie in the compensatory mechanisms to loss of DAT. Indeed, DAT is normally present at higher levels in the SNc and striatum than in the VTA and accumbens (Ciliax *et al*., 1995, Miller *et al*., 1997). Uptake is in fact much more efficient in the striatum than in the accumbens (Cass *et al*., 1992; Nirenberg *et al*., 1996). Therefore, its loss in our animal model induces a higher extracellular level of dopamine in the striatum than in the accumbens (unpublished observation). As a consequence, in an attempt to compensate for this increased amount of extracellular dopamine, TH is decreased in the dorsal striatum to a greater extent than in the accumbens.

In order to investigate whether the modifications in TH expression are specific to this protein, we measured levels of DDC, expressed in catecholamine neurons where it decarboxylates L-DOPA to dopamine, and VMAT that is localized within storage vesicles of monoamines neurons. Our data show that DDC levels were not modified whereas VMAT levels were decreased by 28.7%, to the same extent as the percentage of loss of dopamine neurons. This apparent discrepancy may be due to the fact that DDC is also expressed in blood vessels that may cover weak changes in DDC expression related to the dopamine system. Both VMAT and DDC labelling are mostly due to dopaminergic projections as neither serotonin nor noradrenaline systems present extensive projections to the striatum as demonstrated by serotonin and dopamine β hydroxylase immunohistochemistry (data not shown). In addition, previous studies have shown that 6-OHDA lesions of the SNc completely abolish VMAT expression in the dorsal striatum, again pointing to the dopamine system as the major monoamine in the striatum and validating the use of VMAT and DDC as dopaminergic markers in this brain area (Darchen *et al*., 1989). Thus, our results suggest that in the $DAT^{-/-}$ mice either TH trafficking from the cell bodies to the terminals in the striatum is specifically altered or, more likely, that TH is differently regulated within distinct areas of the dopamine projections.

The distribution of TH within the dorsal striatum itself is heterogeneous. Indeed, most of the dorsal striatum seems to display extremely low TH immunoreactivity as demonstrated using optic microscopy on 60-μm Vibratome sections and semi-thin sections (1 μm), as well as electron microscopy. The remaining TH projections are indistinguishable from normal projections with respect to intensity of labelling and the presence of low and high density vesicles as previously described (Wassef *et al*., 1981; Freund *et al*., 1984; Matteoli *et al*., 1991; Pickel *et al*., 1996). These projections do not originate from the noradrenergic neurons of the locus coeruleus as these neurons do not project to the dorsal striatum, although some projections do reach the accumbens (Hökfelt *et al*., 1994). Furthermore, and as mentioned above, dopamine β hydroxylase immunohistochemistry analysis performed on $DAT^{-/-}$ animals showed no detectable labelling in the dorsal striatum where TH levels were analysed using electron microscopy. These data suggest that the decrease in TH labelling is probably due to a specific and substantial loss in TH expression in the striatum areas with no loss of dopaminergic projections. Because few TH projections seem to be intact, our results further suggest that dopamine neurons and their projections are composed of functionally distinct subsystems as previously proposed (Weiss-Wunder & Chesselet, 1991).

Intrinsic, striatal tyrosine hydroxylase neurons have received little attention. In a recent work, Betarbet *et al*. (1997) have characterized such neurons in the striatum of control and 1-methyl-4-phenyl-1,2,3,6-tetrahydropyridine (MPTP)-treated monkeys, and found them to be increased following treatment. These neurons are small aspiny and bipolar corresponding morphologically to GABAergic interneurons. Interestingly, they were found to coexpress the DAT suggesting that they contain the machinery to be functional dopaminergic neurons. To the best of our knowledge, only two other reports have identified such neurons in the striatum (Dubach *et al*., 1987; Tashiro *et al*., 1989). The conditions of appearance of these neurons and their relative contribution to the nigrostriatal dopaminergic transmission is not yet well understood. In our animal model the TH cell bodies that we detected in the striatum might be significantly contributing to the DA volume transmission, and the subsequent increase in DA levels and locomotor activity.

An interesting contrast can be drawn between $DAT^{-/-}$ mice, in which as little as 5% of normal DA leads to hyperactivity, and patients with Parkinson's disease in whom similarly low levels of DA cause debilitating impairment in locomotion. Our studies suggest that therapeutic strategies aimed at mimicking some of the properties or adaptive changes of $DAT^{-/-}$ mice could prove beneficial to Parkinson's patients (see also Uhl, 1998). These strategies might include high-affinity DAT blockers (Boja *et al*., 1995), alone or in conjunction with agents that increase synthesis and/or retard degradation of DA (Coyle & Snyder, 1969).

Acknowledgements

We would like to thank M.-C. Fournier for expert technical assistance and Dr P. Costet at the transgenic animal facility, University of V. Segalen. Special thanks for Drs C. Le Moine and R. Gainetdinov for careful reading of the manuscript. This work was partly financed by France Parkinson (M.J.) and grants from the NIH # MH-40159 (M.G.C.).

Abbreviations

DAT, dopamine transporter; $DAT^{+/+}$, homozygote; $DAT^{+/-}$, heterozygote; $DAT^{-/-}$, homozygote; DDC, DOPA decarboxylase; HRP, horseradish peroxidase; MPTP, 1-methyl-4-phenyl-1,2,3,6-tetrahydropyridine; OD, optical density; PBS, phosphate-buffered saline; SDS, sodium dodecyl sulphate; SN,

FIG. 6. Ultrastructural features of dopaminergic innervation in the striatum. (A and B) $DAT^{+/+}$ mice. (C and D) $DAT^{-/-}$ mice. (A) The TH-immunoreactive profiles (arrows) are widespread and homogeneously distributed throughout the whole striatum. (B) High magnification of a labelled axon. The immunogold particles are associated with a bouton forming an asymmetric synapse with a dendritic spine (star). The axon contains numerous small synaptic vesicles and some large dense core vesicles (thin arrows). (C) In $DAT^{-/-}$ mice, TH immunolabelling is absent from most of the striatum with few projections remaining normally labelled (arrows) and presenting no alteration in the number of light and dense vesicles as well as in the ultrastructure in general. (D) The TH-positive bouton forms a symmetric synapse into a dendritic shaft (arrow). Ultrastructural features are not modified. Numerous small synaptic vesicles fill the synaptic bouton. Scale bar, 0.5 μm (A–D).

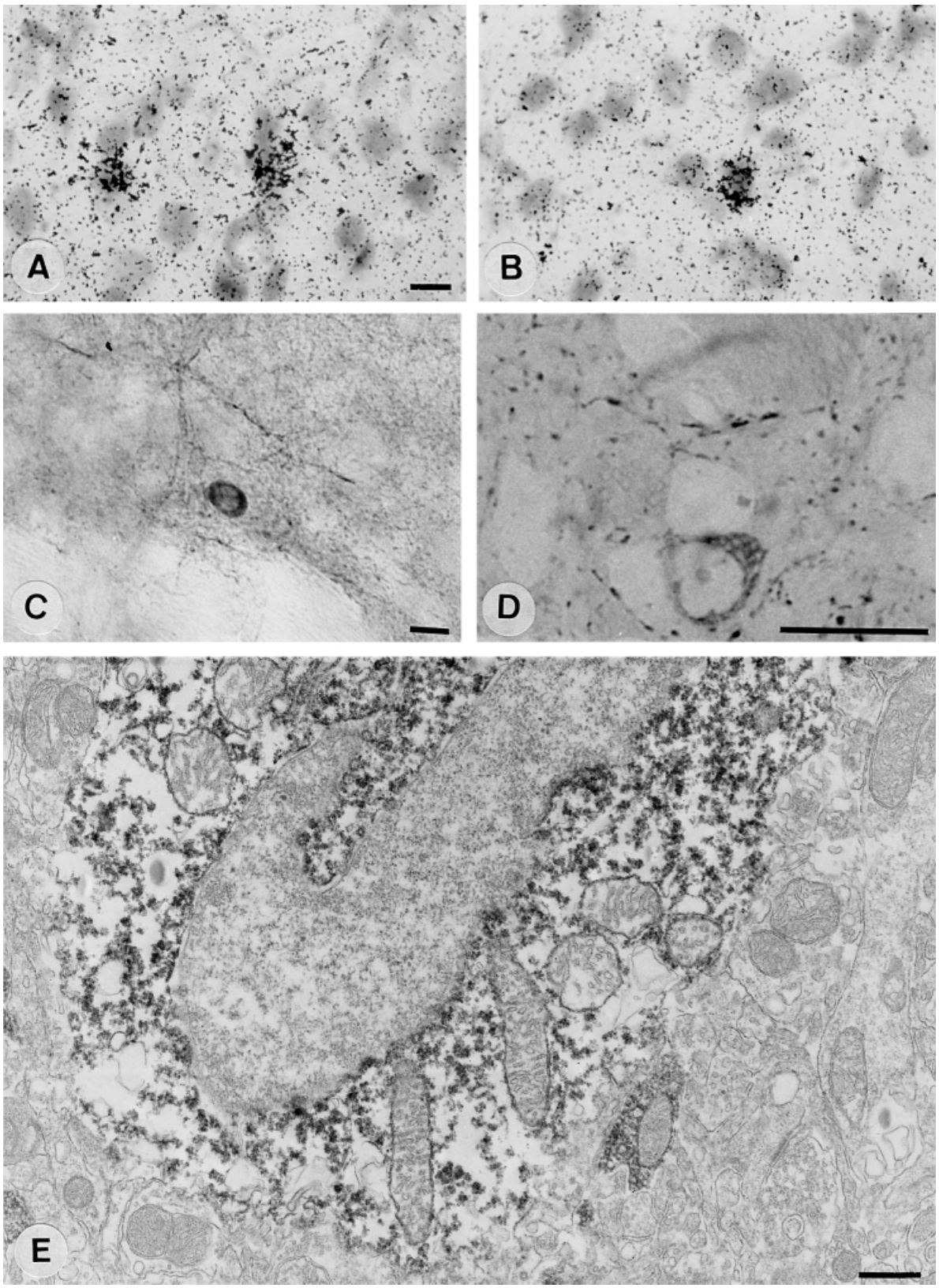

FIG. 7. TH-positive neurons in the striatum of wild-type and homozygote animals. *In situ* hybridization with a probe against TH mRNA revealed the existence of labelled neurons in $DAT^{+/+}$ (A) and $DAT^{-/-}$ animals (B). No significant difference was found in the number of these neurons in $DAT^{+/+}$ and $DAT^{-/-}$ mice, although there was a tendency to an increase in $DAT^{-/-}$ animals. TH-immunoreactive neurons were observed in the striatum of $DAT^{-/-}$ animals on 60-µm Vibratome sections (C) and 1-µm semi-thin sections (D). These neurons are medium sized and were found mainly in the ventral striatum. No such labelling is observed in $DAT^{+/+}$ animals most probably because TH projections from the midbrain are extensively labelled and mask the weak labelling of TH neurons. (E) TH-immunoreactive perikaryon in the striatum. Note that the nucleus exhibits a deep infolding. The peroxidase reaction product diffused over the entire cytoplasm. Scale bar, 20 µm (C and D); 0.5 µm (E).

substantia nigra; TH, tyrosine hydroxylase; VMAT, vesicular monoamines transporter; VMB, ventral midbrain; VTA, ventral tegmental area.

References

Beatriz, A.R., Fumagalli, F., Gainetdinov, R.R., Jones, S.R., Ator, R., Giros, B., Miller, G.W. & Caron, M.G. (1998) Cocaine self-administration in dopamine-transporter knockout mice. *Nature Neurosci.*, **1**, 132–137.

Betarbet, R., Turner, R., Chockkan, V., DeLong, M.R., Allers, K.A., Walters, J., Levey, A.I. & Greenamyre, J.T. (1997) Dopaminergic neurons intrinsic to the striatum. *J. Neurosci.*, **17**, 6761–6768.

Bezard, E., Gross, C.E., Fournier, M.-C., Dovero, S., Bloch, B. & Jaber, M. (1999) Absence of MPTP induced neuronal death in mice lacking the dopamine transporter. *Exp. Neurol.*, **155**, 268–273.

Boja, J.W., Cadet, J.L., Kopajtic, T.A., Lever, J., Seltzman, H.H., Wyrick, C.D., Lewin, A.H., Abraham, P. & Carrol., F.I. (1995) Selective labeling of the dopamine transporter by the high affinity ligand 3b-(4-[^{125}I] iodophenyl) tropane-2b-carboxylic acid isopropyl ester. *Mol. Pharmacol.*, **47**, 779–786.

Bugnon, C., Hadjiyiassemis, M., Fellmann, D. & Cardot, J. (1983) Reserpine-induced depletion of corticoliberin (CRF)-like immunoreactivity in the zona externa of the rat median eminence. *Brain Res.*, **275**, 198–201.

Cass, W.A., Gerhardt, G.A., Mayfield, R.D., Curella, P. & Zahniser, N.R. (1992) Differences in dopamine clearance and diffusion in rat striatum and nucleus accumbens following systemic cocaine administration. *J. Neurochem.*, **59**, 259–266.

Ciliax, B.J., Heilman, C., Demchyshyn, L.L., Pristupa, Z.B., Ince, E., Hersch, S.M., Niznik, H.B. & Levey, A.I. (1995) The dopamine transporter: immunochemical characterization and localization in brain. *J. Neurosci.*, **15**, 1714–1723.

Coyle, J.T. & Snyder, S.H. (1969) Catecholamine uptake by synaptosomes in homogenates of rat brain: stereospecificity in different areas. *J. Pharmacol. Exp. Ther.*, **170**, 221–231.

Darchen, F., Masuo, Y., Vial, M., Rostene, W. & Scherman, D. (1989) Quantitative autoradiography of the rat brain vesicular monoamine transporter using the binding of [3H]dihydrotetrabenazine and 7-amino-8-[125I]iodoketanserin. *Neuroscience*, **33**, 341–349.

Dubach, M., Schmidt, R., Kundel, D., Bowden, D.M., Martin, R. & German, D.C. (1987) Primate neostriatal neurons containing tyrosine hydroxylase: immunohistochemical evidence. *Neurosci. Lett.*, **75**, 205–210.

Franklin, K.B.J. & Paxinos, G. (1997) *The Mouse Brain in Stereotaxic Coordinates*. Academic Press, California, USA.

Freund, T.F., Powell, J.F. & Smith, A.D. (1984) Tyrosine hydroxylase-immunoreactive boutons in synaptic contact with identified striatonigral neurons, with particular reference to dendritic spines. *Neuroscience*, **13**, 1189–1215.

Gainetdinov, R.R., Fumagelli, F., Jones, S.R. & Caron, M.G. (1997) Dopamine transporter is required for *in vivo* MPTP neurotoxicity: evidence from mice lacking the transporter. *J. Neurochem.*, **69**, 1322–1325.

Gainetdinov, R.R., Wetsel, W.C., Jones, S.R., Levin, E.D., Jaber, M. & Caron, M.G. (1999) Role of serotonin in the paradoxical calming effect of psychostimulants on hyperactivity. *Science*, **283**, 397–401.

Giros, B., Sokoloff, P., Martres, M.P., Riou, J.F., Emorine, L.J. & Schwartz, J.C. (1989) Alternative splicing directs the expression of two D2 dopamine receptor isoforms. *Nature*, **342**, 923–926.

Giros, B., El Mestikawy, S., Bertrand, L. & Caron, M.G. (1991) Cloning and functional characterization of a cocaine-sensitive dopamine transporter. *FEBS Lett.*, **295**, 149–154.

Giros, B. & Caron, M.G. (1993) Molecular characterization of the dopamine transporter. *Trends Pharmacol. Sci.*, **14**, 43–49.

Giros, B., Jaber, M., Jones, S.R., Wightman, R.M. & Caron, M.G. (1996) Hyperlocomotion and indifference to cocaine and amphetamine in mice lacking the dopamine transporter. *Nature*, **379**, 606–612.

Grima, B., Lamouroux, A., Blanot, F., Faucon Biguet, N. & Mallet, J. (1985) Complete coding sequence of rat tyrosine hydroxylase mRNA. *Proc. Natl Acad. Sci. USA*, **85**, 617–621.

Hökfelt, T., Johansson, O. & Goldstein, M. (1995) Central catecholamine neurons as revealed by immunohistochemistry with special reference to adrenaline neurons. In Bjorklund, A. & Hökfelt, T. (eds), *Handbook of Chemical Neuroanatomy,* Vol. 2, Part I, *Classical Transmitters in the CNS*. Elsevier Science, Amsterdam, pp. 157–276.

Jaber, M., Normand, E. & Bloch, B. (1995) Effect of reserpine treatment on enkephalin mRNA level in the rat striatum: an in situ hybridization study. *Mol. Brain Res.*, **32**, 156–160.

Jaber, M., Robinson, S.W., Missale, C. & Caron, M.G. (1996) Dopamine receptors and brain function. *Neuropharmacology*, **35**, 1503–1519.

Jaber, M., Jones, S.R., Giros, B. & Caron, M.G. (1997) The dopamine transporter: a crucial component regulating dopamine neurotransmission. *Mov. Disorder*, **12**, 629–633.

Jones, S.R., Gainetdinov, R., Jaber, M., Giros, B., Wightman, R.M. & Caron, M.G. (1998) Profound neuronal plasticity in response to inactivation of the dopamine transporter. *Proc. Natl Acad. Sci. USA*, **95**, 4029–4034.

Jones, S.R., Gainetdinov, R.R., Hu, X.T., Cooper, T.C., Wightman, R.M., White, F.J. & Caron, M.G. (1999) Loss of autoreceptor functions in mice lacking the dopamine transporter. *Nature Neurosci.*, **2**, 649–655.

Kaneda, N., Sasaoka, T., Kobayashi, K., Kiuchi, K., Nagatsu, I., Kurosawa, Y., Fujita, K., Yokoyama, M., Nomura, T., Katsuki, M. & Nagatsu, T. (1991) Tissue-specific and high-level expression of the human tyrosine hydroxylase gene in transgenic mice. *Cell*, **6**, 583–594.

Krieger, M., Tillet, Y., Gros, F. & Thibault, J. (1993) Preparation of antiserum using a fusion protein produced by a cDNA for rat aromatic L-amino acid decarboxylase. *Neurosci. Lett.*, **153**, 88–92.

Kumer, S.C. & Vrana, K.E. (1996) Intricate regulation of tyrosine hydroxylase activity and gene expression. *J. Neurochem.*, **67**, 443–462.

Levitt, M., Spector, S., Sjoerdsma, A. & Udenfriend, S. (1965) Elucidation of the rate-limiting step in norepinephrine biosynthesis in the perfused guinea-pig-heart. *J. Pharmacol. Exp. Ther.*, **148**, 1–7.

Matteoli, M., Reetz, A.T. & De Camilli, P. (1991) Small synaptic vesicles and large dense-core vesicles: secretory organelles involved in two modes of neuronal signaling. In Fuxe, K. & Agnati, L.F. (eds), *Volume Transmission in Brain: Novel Mechanisms for Neuronal Transmission*. Raven Press, New York, pp. 181–193.

Miller, G.W., Staley, J.K., Heilman, C.J., Perez, J.T., Mash, D.C., Rye, D.B. & Levey, A.I. (1997) Immunochemical analysis of dopamine transporter protein in Parkinson's disease. *Ann. Neurol.*, **41**, 530–539.

Nagatsu, T., Levitt, M. & Udenfriend, A. (1964) Tyrosine hydroxylase, the initial step in norepinephrine biosynthesis. *J. Biol. Chem.*, **239**, 2910–2917.

Nirenberg, M.J., Vaughan, R.A., Uhl, G.R., Kuhar, M.J. & Pickel, V.M. (1996) The dopamine transporter is localized to dendritic and axonal plasma membranes of nigrostriatal dopaminergic neurons. *J. Neurosci.*, **16**, 436–447.

Pasinetti, G.M., Osterburg, H.H., Kelly, A.B., Kohama, S., Morgan, D.G., Reinhard, J.F., Stellwagen, R.H. & Finch, C.E. (1992) Slow changes of tyrosine hydroxylase gene expression in dopaminergic brain neurons after neurotoxin lesioning: a model for neuron aging. *Mol. Brain Res.*, **13**, 63–73.

Pickel, V.M., Nirenberg, M.J. & Milner, T.A. (1996) Ultrastructural view of central catecholaminergic transmission: immunocytochemical localization of synthesizing enzymes, transporters and receptors. *J. Neurocytol.*, **25**, 843–856.

Tanaka, T., Horio, Y., Taketoshi, M., Imamura, I., Ando-Yamamoto, M., Kangawa, K., Matsuo, H., Kuroda & Wada, M.H. (1989) Molecular cloning and sequencing of a cDNA of rat dopa decarboxylase: partial amino acid homologies with other enzymes synthesizing catecholamines. *Proc. Natl Acad. Sci. USA*, **86**, 8142–8146.

Tashiro, Y., Sugimoto, T., Hattori, T., Uemura, Y., Nagatsu, I., Kikuchi, H. & Mizuno, N. (1989) Tyrosine hydroxylase-like immunoreactive neurons in the striatum of the rat. *Neurosci. Lett.*, **97**, 6–10.

Uhl, G.R. (1998) Hypothesis: the role of dopaminergic transporters in selective vulnerability of cells in Parkinson's disease. *Ann. Neurol.*, **43**, 555–560.

Wassef, M., Berod, A. & Sotelo, C. (1981) Dopaminergic dendrites in the pars reticulata of the rat substantia nigra and their striatal input. Combined immunocytochemical localization of tyrosine hydroxylase and anterograde degeneration. *Neuroscience*, **6**, 2125–2139.

Weiss-Wunder, L.T. & Chesselet, M.-F. (1991) Subpopulations of mesencephalic dopaminergic neurons express different levels of tyrosine hydroxylase messenger RNA. *J. Comp. Neurol.*, **303**, 478–488.